

See discussions, stats, and author profiles for this publication at: <https://www.researchgate.net/publication/262816336>

In Vitro Selection of DNA Aptamers for Metastatic Breast Cancer Cell Recognition and Tissue Imaging

ARTICLE *in* ANALYTICAL CHEMISTRY · JUNE 2014

Impact Factor: 5.64 · DOI: 10.1021/ac501205q · Source: PubMed

CITATIONS

14

READS

51

8 AUTHORS, INCLUDING:



Wei Yun Zhang

Xiamen University

20 PUBLICATIONS 343 CITATIONS

[SEE PROFILE](#)



Zhi Zhu

China Medical University (ROC)

171 PUBLICATIONS 3,571 CITATIONS

[SEE PROFILE](#)



Chaoyong James Yang

Xiamen University

123 PUBLICATIONS 4,604 CITATIONS

[SEE PROFILE](#)

In Vitro Selection of DNA Aptamers for Metastatic Breast Cancer Cell Recognition and Tissue Imaging

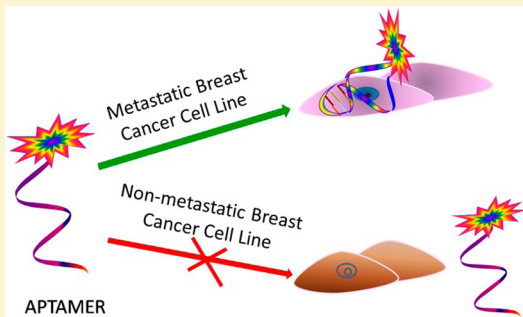
Xilan Li,[†] Weiyun Zhang,^{†,‡} Lu Liu,[†] Zhi Zhu,[†] Gaoliang Ouyang,[‡] Yuan An,[†] Chunyi Zhao,[†] and Chaoyong James Yang^{*,†}

[†]The MOE Key Laboratory of Spectrochemical Analysis and Instrumentation, State Key Laboratory of Physical Chemistry of Solid Surfaces, the Key Laboratory for Chemical Biology of Fujian Province, Department of Chemical Biology, College of Chemistry and Chemical Engineering, Xiamen University, Xiamen, Fujian 361005, P. R. China

[‡]Department of Pharmacy, Xiamen Medical College, Xiamen, Fujian 361008, P. R. China

^{*}State Key Laboratory of Stress Cell Biology, School of Life Sciences, Xiamen University, Xiamen, Fujian 361005, P. R. China

ABSTRACT: Cancer is a major public health issue, with metastatic cancer accounting for the overwhelming majority of cancer deaths. Early diagnosis and appropriate treatment of metastatic cancer may largely prolong the survival rate and improve the quality of life for patients. In this study, we have identified a panel of DNA aptamers specifically binding to MDA-MB-231 cells derived from metastatic site-pleural effusion, with high affinity after 15 rounds of selections using the cell-based systematic evolution of ligands by exponential enrichment (SELEX) method. The selected aptamers were subjected to flow cytometry and laser confocal fluorescence microscopy to evaluate their binding affinity and selectivity. The aptamer LXL-1 with the highest abundance in the enriched library demonstrated a low K_d value and excellent selectivity for the recognition of the metastatic breast cancer cells. Tissue imaging results showed that truncated aptamer sequence LXL-1-A was highly specific to the corresponding tumor tissue and displayed 76% detection rate against breast cancer tissue with metastasis in regional lymph nodes. Therefore, on the basis of its excellent targeting properties and functional versatility, LXL-1-A holds great potential to be used as a molecular imaging probe for the detection of breast cancer metastasis. Our result clearly demonstrates that metastatic-cell-based SELEX can be used to generate DNA ligands specifically recognizing metastatic cancer cells, which is of great significance for metastatic cancer diagnosis and treatment.



Cancer is the leading cause of death worldwide.^{1–4} Early detection and identification of cancer, while still localized and curable, represents a promising approach to reduce the increasing cancer burden.⁵ Detection of stage 1 cancers has been found to correlate with >90% 5-year survival rate in most cases.⁶ Although anatomic imaging represents the mainstay in cancer detection and classification as well as assessment of treatment response, these traditional diagnostic methods based on morphologic criteria mainly image the advanced manifestation of cancer by using nonspecific contrast agents.^{7,8} In contrast, molecular imaging examines the abnormal molecules that are fundamental to neoplasia. Because changes in molecules associated with a tumor can be detected much earlier than changes in tumor size, molecular imaging plays a key role in detecting cancer in its earliest stages.^{6,9} Molecular imaging can be realized by using probes consisting of a targeting ligand and a signaling component.^{7,9} Although the targeting ligands are usually proteins and peptides, aptamers possess enormous potential to become a new alternative in molecular imaging because of their multiple unique properties.^{10,11}

Aptamers are structurally distinct, single-stranded oligonucleotide molecules that can bind strongly and selectively to

their targets.^{12,13} Through a process called systematic evolution of ligands by exponential enrichment (SELEX), aptamer can be enriched and identified from a very large random oligonucleotide library.^{14–18} Aptamers have several advantages over antibodies including the ease of synthesis and modification, high stability, small molecular weight as well as low immunogenicity.^{13,19–22} Therefore, in recent years, researchers have shown tremendous interest in the application of aptamers in molecular medicine, including aptamer-based molecular imaging.^{10,11,23–28} For example, an activatable aptamer probe (AAP) designed by Shi et al. displayed enhanced contrast for *in vivo* cancer imaging because the APP can be activated through conformational alteration in the presence of target cancer cells.²⁹ By conjugating targeting aptamer to paramagnetic molecules such as superparamagnetic iron oxide nanoparticles (SPIONs), magnetic resonance imaging (MRI) has evolved from general anatomical imaging to molecular imaging, including adenosine, thrombin, and prostate cancer detection.^{30–32} A prostate-specific membrane antigen (PSMA)

Received: April 3, 2014

Accepted: June 3, 2014

Published: June 3, 2014

aptamer-gold nanoparticle bioconjugate was also reported for computed tomography (CT) imaging of PSMA-expressing prostate cancer cells.³³ In addition, a study on ^{99m}Tc radiolabeled aptamers against the extracellular matrix protein tenascin-C and MUC1 protein demonstrated the potential application of aptamers in nuclear imaging (i.e., SPECT and PET) for tumor imaging.^{34,35}

However, so far, very few aptamer probes have been reported in molecular imaging of metastatic cancer. It is well-known that metastatic cancer with poor prognosis cannot be cured and account for the majority of cancer deaths. It is of great importance to develop molecular ligands that can specifically recognize metastatic cancer cells for earlier diagnosis and appropriate treatment of metastatic cancer.

In this study, we have identified DNA aptamers that can bind selectively to metastatic tumor cells with high affinity. Cell-SELEX was used to identify new aptamers with high affinity and specificity for breast cancer cells MDA-MB-231 derived from metastatic site, pleural effusion, using normal breast cells MCF-10A as control. The selected aptamers were subjected to flow cytometry and laser confocal fluorescence microscopy to evaluate their binding affinity and selectivity. The aptamer LXL-1 with highest abundance in the enriched library demonstrated a low K_d value and excellent selectivity for the recognition of the metastatic breast cancer cells. Tissue imaging results showed that truncated aptamer sequence LXL-1-A was highly specific to the corresponding tumor tissue and displayed 76% detection rate against breast cancer tissue with metastasis in regional lymph nodes.

EXPERIMENTAL SECTION

Cell Lines and Cell Culture. Human breast cancer cells MDA-MB-231, MDA-MB-453, MCF-7, and human normal epithelium cells MCF-10A were obtained from the American Type Culture Collection (ATCC). Human cervical cancer cell line HeLa, human liver cancer cell lines QGY-7703 and HepG2, and human normal liver cell line QSG-7701 were purchased from the Cell Bank of Chinese Academy of Science (Shanghai, China). Human breast cancer cells T47D were a gift from Professor Wei Duan of Deakin University, Australia. All cell lines were maintained at 37 °C in a humid atmosphere with 5% CO₂. MDA-MB-231, MCF-7, T47D, QGY-7703, and QSG-7701 were cultured in RPMI-1640 supplemented with 10% fetal bovine serum (FBS) and 100 U/mL penicillin-streptomycin. MDA-MB-453, HeLa, and HepG2 were cultured in DMEM supplemented with 10% FBS and 100 U/mL penicillin-streptomycin. The growth medium for MCF-10A contained DMEM/F12 supplemented with 5% horse serum, 20 ng/mL epidermal growth factor, 10 µg/mL insulin, 0.5 µg/mL hydrocortisone, 100 ng/mL cholera toxin, and penicillin-streptomycin as described in the literature.

SELEX Library and Primers. The initial library used in our previous study was used in this work.³⁶ The library comprised a randomized region of 45 (N45) nucleotides flanked on both sides by two constant regions for primer annealing and PCR amplification (5'-GAA TTC AGT CGG ACA GCG-N45-GAT GGA CGA ATA TCG TCT CCC-3'). For PCR amplification, forward primer, 5'-FAM or Cy5-GAA TTC AGT CGG ACA GCG-3', and reverse primer, 5'-Biotin-GGG AGA CGA TAT TCG TCC ATC-3', were used. All of the oligonucleotide synthesis services were provided by Shanghai Sangon Biotech Co., Ltd. China.

SELEX Procedures. In this study, human breast cancer cells MDA-MB-231 were used as the target cell line. In 500 µL of binding buffer (4.5 g/L glucose, 5 mM MgCl₂, 0.1 mg/mL yeast tRNA, and 1 mg/mL BSA in PBS, pH 7.4), 5 nmol of DNA library was dissolved thoroughly and used as the initial library. After being denatured at 95 °C for 5 min and immediately cooled on ice for 10 min, the initial library was incubated with 5 × 10⁶ MDA-MB-231 cells for 1 h on ice in a 100 mm × 20 mm culture dish. After being washed with 3 mL of washing solution (4.5 g/L glucose, 5 mM MgCl₂ in PBS, pH 7.4) for 30 s at 120 rpm, cells were harvested and transferred to 500 µL of water. The mixture was heated at 95 °C for 5 min to elute bound DNA sequences from the cell surface, which were amplified by PCR with FITC labeled forward primer and biotin labeled reverse primers (5–15 cycles of 30 s at 94 °C, 30 s at 49.5 °C, and 30 s at 72 °C, followed by 5 min at 72 °C). The amplified double-stranded DNA product was then captured on streptavidin-coated sepharose beads (GE Healthcare). After treating with 0.2 M NaOH, the selected sense ssDNA was separated from the biotinylated antisense ssDNA strand and used for the next round selection.

Starting from the second round, the DNA library was first incubated with negative cells MCF-10A (5 × 10⁶ cells) on ice for 30 min as a counter selection to remove nonspecific cell binding sequences. The eluted DNAs were then incubated with MDA-MB-231 cells. In the first round of selection, only positive selection was performed. To increase the stringency of the selection, the positive incubation time was shortened from 60 to 30 min as the number of selection rounds increased, and the washing time was also extended gradually from 30 to 60 s. At the same time, negative incubation time was gradually increased from 30 to 60 min. Especially with the 10th round, more than two successive controls were performed during the enrichment process in order to maximize the removal of ssDNA binding with control cells. In addition, 10% FBS was included in the incubation mixture after the third round of selection.

Flow Cytometry Analysis of Enrichment Pools. To monitor the enrichment, the FAM-labeled ssDNA pools at a final concentration of 250 nM were incubated with 2 × 10⁵ cells on ice for 30 min. After washing with 500 µL of washing buffer three times, cells were resuspended in 200 µL of washing buffer. The fluorescence intensity was recorded in triplicate by a FACScan cytometer (Becton Dickinson Immunocytometry Systems) by counting 10 000 events. The initial ssDNA library was used as a negative control.

Cloning and DNA Sequencing of Enriched Pools. Selection was completed when a significant difference was observed between the fluorescence signal intensity of the selected pools and the control background. The resulting pool from the 15th round was PCR amplified, cloned, and sequenced (Genomics Institute, Beijing). The resulting 100 sequences were analyzed by Clustal X 2.0.3 software to identify highly conserved motifs in the group of selected DNA sequences.³⁷ Sequences with high repeats were chemically synthesized for further study.

Evaluation of Selectivity of Aptamers. To investigate the recognition of all the selected aptamers, positive cell line MDA-MB-231, negative cell line MCF-10A, and other related breast cancer cell lines MCF-7, MDA-MB-453, and T47D were incubated with FAM-labeled aptamers for binding assays by flow cytometry. To test the selectivity against other types of cells, cervical cancer cell line HeLa, human normal liver cell line

QSG-7701, and human liver cancer cell lines QGY-7703 and HepG2 were also tested.

Binding Analysis. The aptamer binding affinities were determined by incubating MDA-MB-231 cells (1×10^6) on ice for 30 min in the dark with various concentrations of FAM-labeled aptamer in 200 μL of binding buffer. Cells were then washed three times with 500 μL of washing buffer, resuspended in 200 μL of binding buffer, and subjected to flow cytometric analysis. The FAM-labeled initial DNA library was used as negative control to determine nonspecific binding. All of the experiments for the binding assay were repeated three times. By fitting the dependence of fluorescence intensity of cell/aptamer complex on aptamer concentration with the equation $Y = B_{\max}X/(K_d + X)$ using SigmaPlot software (Jandel Scientific), the dissociation constant (K_d) of the aptamer-cell binding was determined.

Proteinase Treatment. Target cells MDA-MB-231 (1×10^6) were washed with 1 mL of PBS and then exposed to 200 μL of 0.05% trypsin/0.53 nM EDTA in PBS at 37 °C for 0.5 or 1 min. FBS was then added to inhibit proteinase before washing the cells with 2 mL of binding buffer. Binding affinity of the aptamer to the treated cells was investigated via flow cytometry analysis.

Cell or Tissue Imaging Using Selected Aptamers. Cell treatment steps were the same as those described in Flow Cytometry Analysis of Enrichment Pools. The tissue microarray was obtained from US Biomax (Xi'an AiLiNa Biotechnology Co., Ltd. China). Tissue pretreatment was performed as described in the literature.^{38,39} Briefly, tissue sections were incubated in xylene to remove paraffin (5 min $\times 3$) and then immersed in a degraded ethanol series (100%, 95%, 80%, and 70%) each for 5 min to rehydrate. After washing with PBS buffer, the hydrated tissue sections were heated in citrate buffer (0.01 M, pH 6.0) at 95 °C for 2 min to retrieve antigens. The prepared tissue sections blocked with 5% BSA for 60 min were incubated with 250 nM FAM-labeled aptamer in 200 μL of binding buffer for 30 min on ice in the dark. A Leica TCS SPS microscope (Leica Microsystems CMS GmbH, Germany) was used for imaging.

RESULTS AND DISCUSSION

Selection of DNA Aptamer against Metastatic Breast Cancer Cell Line MDA-MB-231. For generating aptamers against metastatic breast cancer cells, human breast cancer cell line MDA-MB-231 derived from metastatic site pleural effusion was used as target cells with normal human mammary epithelial cell line MCF-10A as negative control. The cell-SELEX process is schematically shown in Figure 1. After the first round, the DNA library was incubated first with negative MCF-10A cells to remove nonspecific sequences. The unbound DNA was collected and then incubated with target MDA-MB-231 cells for positive selection. After washing, the bound DNA was eluted and amplified for next-round selection. After the last round of selection, the enriched DNA library was cloned and sequenced for identification of individual sequence information.

The enrichment of the aptamer selection process was monitored using flow cytometry. The fluorescence intensity of the labeled cells represented the binding capability of FAM-labeled DNA library to the MDA-MB-231. With an increasing number of selection rounds, steady increases in fluorescence intensity on the target cells were observed (Figure 2A), suggesting that DNA sequences with better binding affinity to MDA-MB-231 cells were enriched. In contrast, almost no

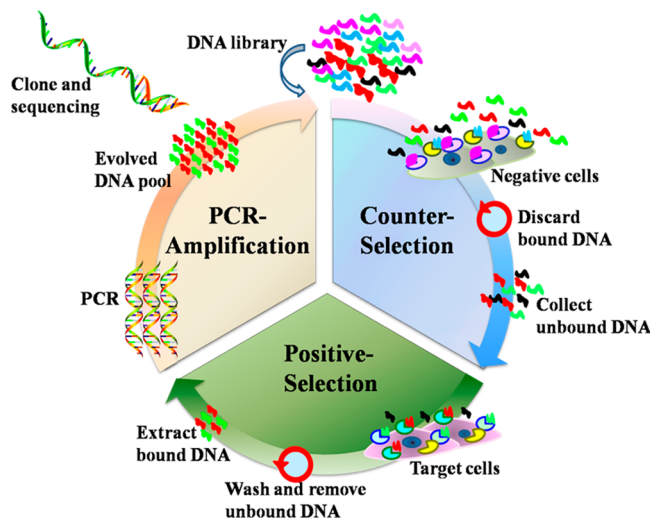


Figure 1. Schematic representation of systematic enrichment of aptamers against metastatic breast cancer cell MDA-MB-231. The DNA library was incubated with MCF-10A cells (negative cells) for counter selection to remove nonspecific sequences. The unbound DNAs were collected and then incubated with MDA-MB-231 cells (target cells) for positive selection. After washing, the bound DNAs were eluted and amplified by PCR for next-round selection. After the library was enriched, DNA cloning and sequencing were used to identify individual aptamer sequences.

increase in fluorescence signal was observed with the MCF-10A cells (Figure 2B), indicating that the binding of enriched pools was specific to MDA-MB-231 cells. The decrease in fluorescence signal of the control cells from the 10th to 14th rounds may be the result of performing more than two successive counter selections on each round to enhance the specificity of the enriched library. After 15 rounds of selection, the enriched DNA pool was cloned and sequenced.

Affinity of DNA Aptamer Candidates to Metastatic Breast Cancer Cells. In order to identify individual aptamer candidates, 100 positive clones of the enriched library were sequenced. The sequencing data was analyzed with Clustal X 2.0.3.³⁷ The sequences were mainly grouped into seven families based on the homology of the DNA sequences of individual clones with each group containing the same motifs. The number of sequences in the distinct homologous families ranged from 1 to 39. Sequences with abundance over 3% were chosen and synthesized for further analysis. The selected six representative sequences LXL-1, LXL-4, LXL-7, LXL-9, LXL-14, and LXL-37 accounted for 39%, 4%, 6%, 6%, 5%, and 4% of all identified sequences, respectively. The binding abilities of the selected sequences to target cells were evaluated by flow cytometry. As shown in Figure 3 and Table 1, the equilibrium dissociation constant (K_d) values of all six sequences were in the low nanomolar range, from 3 to 108 nM, demonstrating the strong binding of these sequences to target MDA-MB-231 cells.

Selectivity of DNA Aptamer Candidates. To test the selectivity of the aptamer candidates, FAM-labeled aptamers were tested with human normal breast cells MCF-10A and other related breast cancer cell lines including MCF-7 from metastatic site-pleural effusion, MDA-MB-453 from metastatic site-pericardial effusion, and T47D from metastatic site-pleural effusion (Figure 4B–E). All of the aptamers showed significantly higher fluorescence intensity than that of the unselected library against MDA-MB-231 and T47D cell lines,

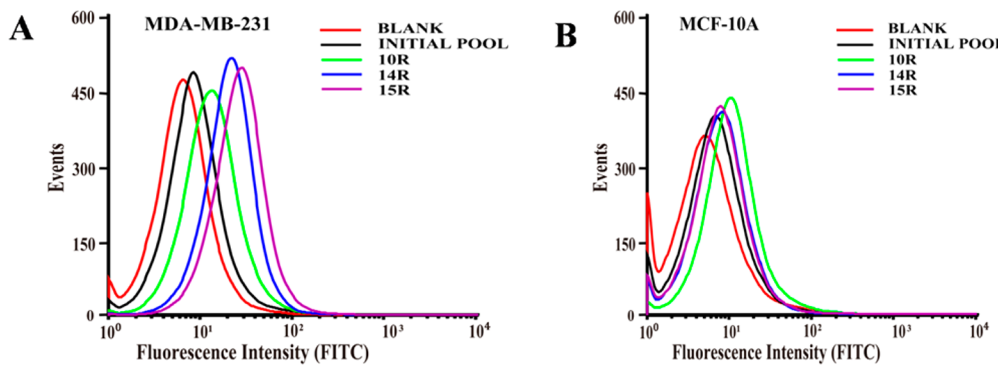


Figure 2. Binding assay of the enriched pool with MDA-MB-231 and MCF-10A cells. For the target cells MDA-MB-231, there was an increase in fluorescence intensity as the selection progressed (A), while there was little change for control cells MCF-10A (B). [Enriched pool] = 250 nM.

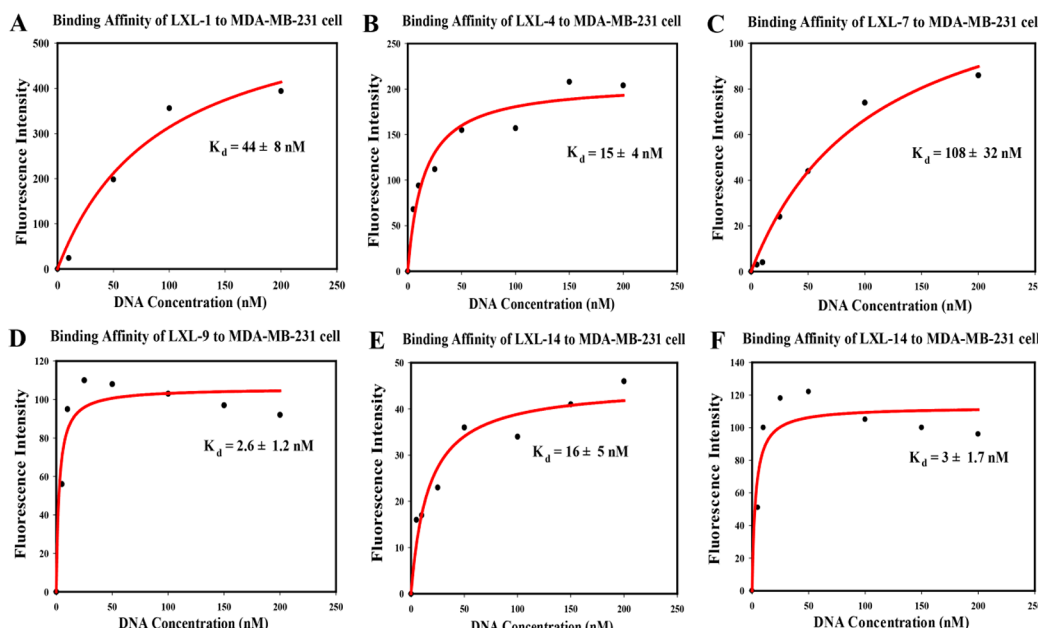


Figure 3. Dissociation constant of selected aptamers for MDA-MB-231. Flow cytometry was used to determine the binding affinities of the FITC-labeled selected aptamer sequences to MDA-MB-231 cells.

Table 1. Sequences and Dissociation Constants (K_d) of Selected Aptamers to MDA-MB-231 Cells

name	sequence	K_d (nM)
LXL-1	GAATTCACTGGACAGCGAAGTAGTTTCCTTCAACCTAACGAAACCCGGCAGTTAATGTAGATGGACGAATACGTCTCCC	44 ± 8
LXL-4	GAATTCACTGGACAGCGCAATTGTGGTTCTACCCCTATCCCTGTGTTGGCGTTGCGATGGACGAATATCGTCTCCC	15 ± 4
LXL-7	GAATTCACTGGACAGCGTAGTAAGAACATCTGTTCTGGCTCTAGCTTGCTGTGTTCTGATGGACGAATATCGTCTCCC	108 ± 32
LXL-9	GAATTCACTGGACAGCGTCAGCGTCCCTTATGCTTGGCTCACCGTCTGAATTCTCAGATGGACGAATATCGTCTCCC	2.6 ± 1.2
LXL-14	GAATTCACTGGACAGCGCGTGAGTCTTGGCTGGCTGGGTCGAATATCTACGACCTGATGGACGAATATCGTCTCCC	19 ± 5
LXL-37	GAATTCACTGGACAGCGTAATCCCTGTGTTGACGTTCAAGATTATTCTATCTTTAGGATGGACGAATATCGTCTCCC	3 ± 1.7

with LXL-1 and LXL-4 having the highest fluorescence signal (Figure 4A,E). Only aptamer LXL-7 showed high affinity for MCF-7 (Figure 4D). These results show that the aptamer against MDA-MB-231 cells derived from metastatic site-pleural effusion is capable not only of distinguishing cells from the different metastatic site-pericardial effusion but also of identifying the subtle difference of these cells from the same metastatic site-pleural effusion. The above results further suggest that the recognition targets of aptamers LXL-1 and LXL-4 are mainly expressed by two metastatic cell lines MDA-MB-231 and T47D, and the target molecule of LXL-7 may be overexpressed by MCF-7 cell lines. Although these aptamers were generated using a breast cancer cell line, the possibility of

recognizing other types of cancers could not be excluded. Therefore, the selectivity was further tested with other types of cell lines, including cervical cancer cell line HeLa (Figure 4I), human normal liver cell line QSG-7701 (Figure 4F), and human liver cancer cell lines QGY-7703 (Figure 4G) and HepG2 (Figure 4H). Except for the recognition of HepG2 by aptamer LXL-4, there was no observable signal with any of the tested cell lines. These results imply that the vast majority of generated aptamers are specific to breast cancers, especially to MDA-MB-231 and T47D cell lines. The selective cell recognition by the aptamers was further confirmed by confocal imaging using Cy5-labeled aptamers. As shown in Figure 5, bright fluorescence was observed on the periphery of the MDA-

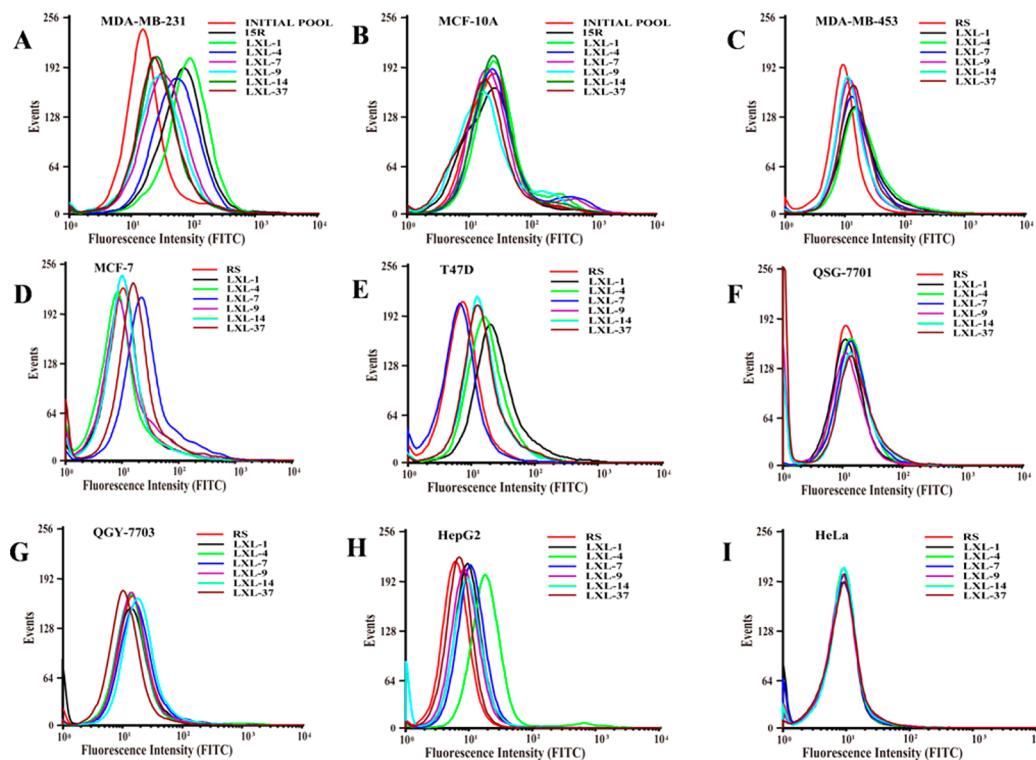


Figure 4. Flow cytometry assay for the binding of the FAM-labeled selected aptamer sequences with MDA-MB-231 cells (A), MCF-10A cells (B), MDA-MB-453 cells (C), MCF-7 cells (D), T47D cells (E), QSG-7701 cells (F), QGY-7703 cells (G), HepG2 cells (H), and HeLa cells (I). [Aptamer] = 250 nM.

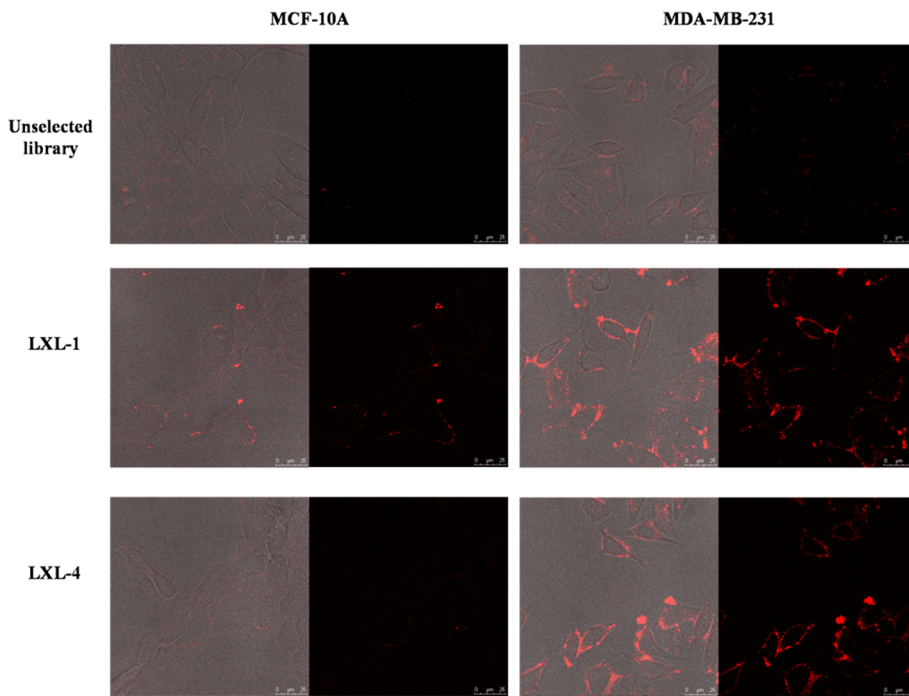


Figure 5. Confocal images of normal and breast cancer cells staining with aptamer LXL-1, LXL-4, and the unselected library. Cells were incubated with Cy5-labeled aptamers and the unselected library. [LXL-1] = [LXL-4] = 250 nM.

MB-231 cells after incubation with aptamers, with no obvious fluorescence observed from the MCF-10A cells. None of the MDA-MB-231 and MCF-10A cells displayed any significant fluorescence signal after incubation with the unselected DNA library. These results demonstrate that aptamers can selectively recognize MDA-MB-231 cells.

Determination of Target Type for Aptamer LXL-1.

Because of its excellent binding affinity and selectivity, aptamer LXL-1 was further characterized and optimized. To check whether the binding target of LXL-1 is an extracellular membrane protein, binding affinity of LXL-1 against trypsin treated cells was investigated. After treating cells with trypsin

for 0.5 min, as shown in Figure 6, LXL-1 lost its binding ability. Binding capacity of LXL-1 further decreased with longer trypsin

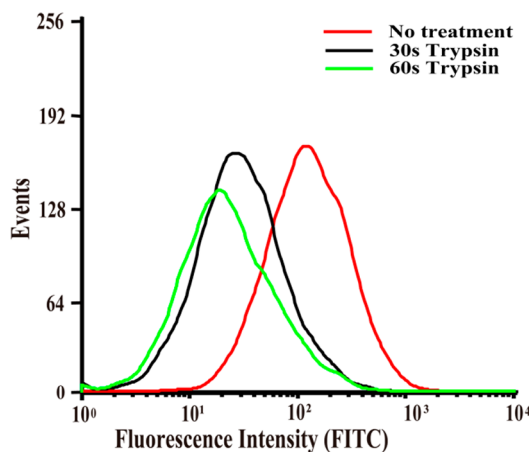


Figure 6. Binding of FAM labeled aptamer LXL-1 to trypsin-treated MDA-MB-231 cells. [LXL-1] = 250 nM.

digestion time. This significant loss of binding efficiency after treatment with trypsin suggests that the binding targets of LXL-1 are most probably extracellular proteins.

Sequence Optimization of Aptamer LXL-1. According to its secondary structure analyzed by NUPACK⁴⁰ (Figure 7A),

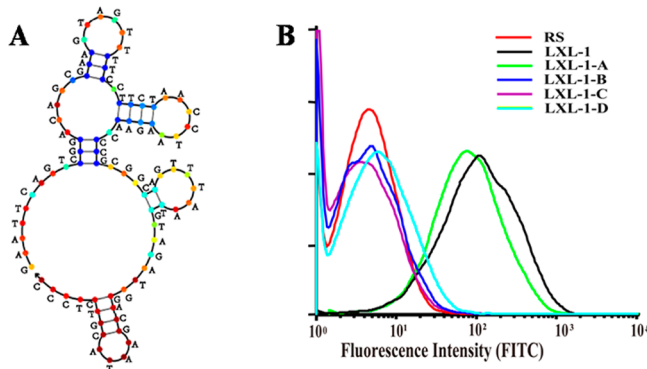


Figure 7. (A) Secondary structure analysis of aptamer LXL-1 predicted by NUPACK. (B) The binding of its four truncated sequences with the target cell line MDA-MB-231.

we optimized the sequence of LXL-1 by gradually truncating its marginal sequence, such as all or part of the primers. Four truncated sequences LXL-1-A, LXL-1-B, LXL-1-C, and LXL-1-D are shown in Table 2. A subsequent aptamer binding assay showed that only LXL-1-A has similar binding to MDA-MB-

Table 2. Truncated Sequences from Aptamer LXL-1

name	sequence
LXL-1-A	GAA TTC AGT CGG ACA GCG AAG TAG TTT TCC TTC TAA CCT AAG AAC CCG CGG CAG TTT AAT GTA GAT GGA CGA A
LXL-1-B	GG ACA GCG AAG TAG TTT TCC TTC TAA CCT AAG AAC CCG CGG CAG TTT AAT GTA GAT GGA CGA ATA CGT CTC CC
LXL-1-C	AAG TAG TTT TCC TTC TAA CCT AAG AAC CCG CGG CAG TTT AAT GTA GAT GGA CGA ATA CGT CTC CC
LXL-1-D	GAA TTC AGT CGG ACA GCG AAG TAG TTT TCC TTC TAA CCT AAG AAC CCG CGG CAG TTT AAT GTA

231 cells compared to the original LXL-1 (Figure 7B). LXL-1-B and LXL-1-C hardly bound to MDA-MB-231 cells, indicating that the forward primer is an indispensable part of the aptamer for binding with target cells by forming a stem-loop structure. Without reverse primer, LXL-1-D lost the ability to recognition to target cell MDA-MB-231. The difference in the binding affinity of LXL-1-A and LXL-1-D suggests that part of the reverse primer contributes to the identification capability of aptamer to target cells.

Imaging of Metastatic Breast Cancer Tissues with Aptamer.

Since the target cells MDA-MB-231 were derived from metastatic site-pleural effusion, we speculated whether the truncated aptamer sequence LXL-1-A has specific recognition to metastatic breast cancer tissue. Laser confocal fluorescence microscopy was used to image metastatic breast cancer tissues with FAM-labeled LXL-1-A to obtain visible images and statistical results (Figure 8 and Table 3). Obviously, the breast cancer tissue with metastasis in regional lymph nodes displayed bright fluorescence after incubation with FAM-labeled LXL-1-A (Figure 8, A1–A8), while breast cancer tissue without regional lymph node metastasis (Figure 8, B1–B4), normal breast tissue (Figure 8, C1–C4), or FAM-labeled random DNA incubated with the breast cancer tissue with metastasis in regional lymph nodes (Figure 8, D1–D4) exhibited negligible fluorescence signal. There was a 76% positive rate among 34 breast cancer tissue with metastasis in regional lymph nodes, 39% positive rate among 38 breast cancer tissues with no regional lymph node metastasis, and 8% positive rate among 12 normal breast tissue or cancer adjacent normal breast tissue (Table 3). These results clearly illustrate that LXL-1-A was highly specific to the corresponding metastatic tumor tissues. Physicians usually prescribe a cancer treatment based on the stage of cancer according to the TNM classification of malignant tumors. The N in TNM stands for the degree of spread to nearby lymph nodes, which means there is a higher risk of postoperative recurrence when cancer has spread to lymph nodes. Traditionally, doctors take needle biopsies on enlarged lymph nodes to determine the presence of cancer cells by observation under the microscope. This method is highly dependent on the experience of a pathologist. It would be very conducive to design a suitable treatment, as well as accurate prognosis and evaluation of therapeutic effect, if molecular-based diagnosis could be performed. Therefore, LXL-1-A has potential as an effective molecular diagnostic reagent for recognizing metastatic breast tumor tissue, a capability of great significance in breast cancer diagnosis and treatment.

CONCLUSIONS

In summary, we have successfully identified a panel of aptamers that selectively bind to MDA-MB-231 cells by cell-SELEX after 15 rounds of enrichment. The K_d values of these developed aptamers are in the lower nanomolar range. The generated aptamers can recognize a subtle difference between the cells from different metastatic sites, pleural effusion, and pericardial effusion, respectively. The target of aptamer LXL-1 with the best recognition and selectivity has been preliminarily determined as membrane protein on the cell surface. Structural studies resulted in a truncated sequence LXL-1-A with the same recognition capability to target cell MDA-MB-231 as LXL-1. Tissue imaging results showed that LXL-1-A was highly specific to the corresponding tumor tissue and displayed a 76% detection rate against metastatic breast cancer tissue. These results suggest that LXL-1-A holds potential to become a

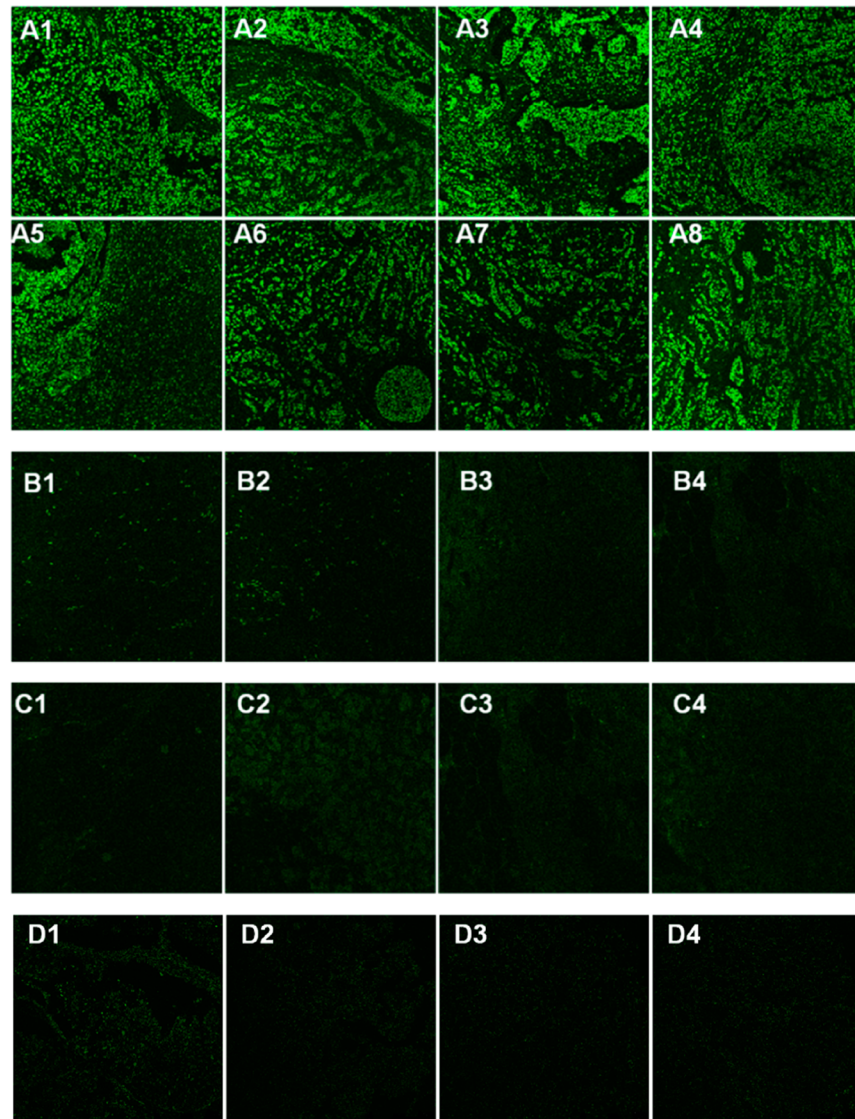


Figure 8. Fluorescence images of tissue sections stained with FAM-labeled LXL-1-A. (A1–A8) Breast cancer tissue with metastasis in regional lymph nodes with LXL-1-A, (B1–B4) breast cancer tissue without regional lymph node metastasis with LXL-1-A, (C1–C4) normal breast tissue with LXL-1-A, and (D1–D4) breast cancer tissue with metastasis in regional lymph nodes with random DNA. [LXL-1-A] = [random DNA] = 250 nM.

Table 3. Tissue Imaging Results Using LXL-1-A

tissue section	number of tissue samples	positive rate, %
breast cancer tissue with metastasis in one or more regional lymph nodes	34	76
breast cancer tissue with no regional lymph node metastasis	38	39
normal breast tissue or cancer adjacent normal breast tissue	12	8

molecular imaging probe for early detection of cancer metastasis. Our results clearly demonstrate that metastatic-cell-based SELEX can be used to generate DNA ligands specifically recognizing metastatic cancer cells, which is of great significance for metastatic cancer diagnosis and treatment.

AUTHOR INFORMATION

Corresponding Author

*E-mail: cyyang@xmu.edu.cn.

Notes

The authors declare no competing financial interest.

ACKNOWLEDGMENTS

We thank the National Basic Research Program of China (2010CB732402, 2013CB933703), the National Science Foundation of China (91313302, 21205100, 21275122, 21075104), National Instrumentation Program (2011YQ03012412), the Fundamental Research Funds for the Central Universities (2012121025), NFFTBS(J1030415), and the National Science Foundation for Distinguished Young Scholars of China (21325522) for their financial support.

REFERENCES

- (1) Jemal, A.; Siegel, R.; Xu, J.; Ward, E. *Ca-Cancer J. Clin.* **2010**, *60*, 277–300.
- (2) Jemal, A.; Bray, F.; Center, M. M.; Ferlay, J.; Ward, E.; Forman, D. *Ca-Cancer J. Clin.* **2011**, *61*, 69–90.
- (3) Siegel, R.; Naishadham, D.; Jemal, A. *Ca-Cancer J. Clin.* **2013**, *63*, 11–30.

- (4) American Cancer Society. *Cancer Facts & Figures 2013*; American Cancer Society: Oklahoma City, Oklahoma, 2013.
- (5) Etzioni, R.; Urban, N.; Ramsey, S.; McIntosh, M.; Schwartz, S.; Reid, B.; Radich, J.; Anderson, G.; Hartwell, L. *Nat. Rev. Cancer* **2003**, *3*, 243–252.
- (6) Weissleder, R. *Science* **2006**, *312*, 1168–1171.
- (7) Kircher, M. F.; Hricak, H.; Larson, S. M. *Mol. Oncol.* **2012**, *6*, 182–195.
- (8) Hussain, T.; Nguyen, Q. T. *Adv. Drug Delivery Rev.* **2014**, *66*, 90–100.
- (9) Blasberg, R. G. *Mol. Cancer Ther.* **2003**, *2*, 335–343.
- (10) Wang, A. Z.; Farokhzad, O. C. *J. Nucl. Med.* **2014**, *55*, 353–356.
- (11) Hong, H.; Goel, S.; Zhang, Y.; Cai, W. *Curr. Med. Chem.* **2011**, *18*, 4195–4205.
- (12) Jayasena, S. D. *Clin. Chem.* **1999**, *45*, 1628–1650.
- (13) Sefah, K.; Shangguan, D.; Xiong, X.; O'Donoghue, M. B.; Tan, W. *Nat. Protoc.* **2010**, *5*, 1169–1185.
- (14) Ellington, A. D.; Szostak, J. W. *Nature* **1990**, *346*, 818–822.
- (15) Tuerk, C.; Gold, L. *Science* **1990**, *249*, 505–510.
- (16) Hu, J.; Wu, J.; Li, C.; Zhu, L.; Zhang, W. Y.; Kong, G.; Lu, Z.; Yang, C. *J. ChemBioChem* **2011**, *12*, 424–430.
- (17) Wu, J.; Wang, C.; Li, X.; Song, Y.; Wang, W.; Li, C.; Hu, J.; Zhu, Z.; Li, J.; Zhang, W.; Lu, Z.; Yang, C. *J. PLoS One* **2012**, *7*, 28.
- (18) Zhang, W. Y.; Zhang, W.; Liu, Z.; Li, C.; Zhu, Z.; Yang, C. *J. Anal. Chem.* **2011**, *84*, 350–355.
- (19) Osborne, S. E.; Matsumura, I.; Ellington, A. D. *Curr. Opin. Chem. Biol.* **1997**, *1*, 5–9.
- (20) Famulok, M.; Hartig, J. S.; Mayer, G. *Chem. Rev.* **2007**, *107*, 3715–3743.
- (21) Hu, M.; Zhang, K. *Future Oncol.* **2013**, *9*, 369–376.
- (22) Saini, K. S.; Taylor, C.; Ramirez, A.-J.; Palmieri, C.; Gunnarsson, U.; Schmoll, H. J.; Dolci, S. M.; Ghenne, C.; Metzger-Filho, O.; Skrzypski, M.; Paesmans, M.; Ameye, L.; Piccart-Gebhart, M. J.; de Azambuja, E. *Anal. Chem.* **2012**, *23*, 853–859.
- (23) Tan, W.; Donovan, M. J.; Jiang, J. *Chem. Rev.* **2013**, *113*, 2842–2862.
- (24) Bouchard, P. R.; Hutabarat, R. M.; Thompson, K. M. *Annu. Rev. Pharmacol. Toxicol.* **2010**, *50*, 237–257.
- (25) Iliuk, A. B.; Hu, L.; Tao, W. A. *Anal. Chem.* **2011**, *83*, 4440–4452.
- (26) Song, Y.; Zhu, Z.; An, Y.; Zhang, W.; Zhang, H.; Liu, D.; Yu, C.; Duan, W.; Yang, C. *J. Anal. Chem.* **2013**, *85*, 4141–4149.
- (27) Zhu, L.; Li, C.; Zhu, Z.; Liu, D.; Zou, Y.; Wang, C.; Fu, H.; Yang, C. *J. Anal. Chem.* **2012**, *84*, 8383–8390.
- (28) Wu, C.; Hu, J.; Zou, Y. A.; Wang, C.; Liu, J.; Yang, C. *J. Prog. Chem.* **2010**, *22*, 1518–1530.
- (29) Shi, H.; He, X.; Wang, K.; Wu, X.; Ye, X.; Guo, Q.; Tan, W.; Qing, Z.; Yang, X.; Zhou, B. *Proc. Natl. Acad. Sci. U. S. A.* **2011**, *108*, 3900–3905.
- (30) Xu, W.; Lu, Y. *Chem. Commun.* **2011**, *47*, 4998–5000.
- (31) Wang, A. Z.; Bagalkot, V.; Vasiliou, C. C.; Gu, F.; Alexis, F.; Zhang, L.; Shaikh, M.; Yuet, K.; Cima, M. J.; Langer, R. *ChemMedChem* **2008**, *3*, 1311–1315.
- (32) Yigit, M. V.; Mazumdar, D.; Lu, Y. *Bioconjugate Chem.* **2008**, *19*, 412–417.
- (33) Kim, D.; Jeong, Y. Y.; Jon, S. *ACS Nano* **2010**, *4*, 3689–3696.
- (34) Winnard, P. T.; Pathak, A. P.; Dhara, S.; Cho, S. Y.; Raman, V.; Pomper, M. G. *J. Nucl. Med.* **2008**, *49*, 96S–112S.
- (35) Pieve, C. D.; Perkins, A. C.; Missailidis, S. *Nucl. Med. Biol.* **2009**, *36*, 703–710.
- (36) Kang, D.; Wang, J.; Zhang, W.; Song, Y.; Li, X.; Zou, Y.; Zhu, M.; Zhu, Z.; Yang, C.; Wahdat, L. T. *PLoS One* **2012**, *7*, No. e42731.
- (37) Thompson, J. D.; Gibson, T. J.; Plewniak, F.; Jeanmougin, F.; Higgins, D. G. *Nucleic Acids Res.* **1997**, *25*, 4876–4882.
- (38) Zhao, Z.; Xu, L.; Shi, X.; Tan, W.; Fang, X.; Shangguan, D. *Analyst* **2009**, *134*, 1808–1814.
- (39) Chen, H. W.; Medley, C. D.; Sefah, K.; Shangguan, D.; Tang, Z.; Meng, L.; Smith, J. E.; Tan, W. *ChemMedChem* **2008**, *3*, 991–1001.
- (40) Zadeh, J. N.; Steenberg, C. D.; Bois, J. S.; Wolfe, B. R.; Pierce, M. B.; Khan, A. R.; Dirks, R. M.; Pierce, N. A. *J. Comput. Chem.* **2011**, *32*, 170–173.